Tribology International 74 (2014) 7–19

Contents lists available at ScienceDirect

Tribology International

journal homepage: www.elsevier.com/locate/triboint

Film thickness in grease lubricated slow rotating rolling bearings

G.E. Morales-Espejel [a,b,*], P.M. Lugt [a,c], H.R. Pasaribu [a,1], H. Cen [c]

[a] SKF Engineering & Research Centre, Nieuwegein, The Netherlands
[b] Université de Lyon, INSA-Lyon, CNRS LaMCoS UMR5259, F69621, Lyon, France
[c] University of Twente, Enschede, The Netherlands

ARTICLE INFO

Article history:
Received 12 October 2013
Received in revised form
20 January 2014
Accepted 22 January 2014
Available online 5 February 2014

Keywords:
Rolling bearings
Grease lubrication
Slow rotation
Large-size bearings

ABSTRACT

Film thickness measurements in grease lubricated contacts are presented for different greases. The conditions used in the experiments are similar to the ones expected in fully-flooded slow rotating bearings. The results show that at very low speeds grease produces film thicknesses substantially thicker than base oil lubrication. An empirical model is developed which can reflect this behaviour. Input to the model is a simple film thickness measurement test to characterise new grease. The model is used to estimate the effective grease viscosity leading to the bearing lubrication parameter kappa. This model is proposed for fully-flooded slow rotating bearings instead of the current practice using the base-oil viscosity.

1. Introduction

Lubrication in rolling bearings is essential for proper operation, for low friction and long life of these machine elements. Soon after the discovery of the Elastohydrodynamic lubrication (EHL) mechanism by Ertel [1] (often attributed to Grubin [2]), engineers have tried to include lubrication in the models for rolling bearing life. It was Dawson [49] who initially proposed a link between the relative film thickness (defined by him as the ratio between the roughness and the lubricating film thickness) and the ability of the contacting surface to withstand pitting. Early attempts to include concepts from EHL and surface topography in rolling bearing life calculations are due to Tallian et al. [3–6]. Liu et al. [5] proposed a sigmoid curve to relate L_{10} bearing life with the lubrication quality parameter known as lambda ($\Lambda = h/R_q$), the results were experimentally confirmed by Skurka [7] and Danner [8]. This work resulted in the adoption of the lubrication parameter (Λ) by the bearing industry [9] and the engineering community [10]. Adréason and Snare [11] introduced the lubrication parameter known as kappa ($\kappa = \nu/\nu_1$) for rolling bearings to calculate the required viscosity of the bearing ν_1 as a function of the speed (n) and bearing mean diameter (d_m). This parameter was initially defined as the ratio between the actual viscosity and the required viscosity by the bearing to have $\Lambda = 1$ and it was linked to a bearing life modifying factor to account for lubrication effects in bearing life. Bolton [12] also published the same diagram and the equations behind the required viscosity. The influence of lubrication in bearing life has also been re-examined by Heemskerk [13]. A later, more up-to-date definition of κ and the bearing life modifying factors is due to Ioannides et al. [14] where lubrication and solid contamination effects were linked to global or average stress concentration factors in the bearing. This methodology was adopted by ISO recently [15], in which the definition of κ is stated as the ratio between the actual viscosity (ν) and a reference viscosity (ν_1) to obtain adequate lubrication conditions. Presently, with the help of powerful computational methods in micro-EHL it is possible to describe in more detail lubrication and surface topography effects in bearing life [16,17].

Early rolling bearing endurance tests were all carried out with grease lubrication, since the test rigs involved are simpler in their design by avoiding an oil circulation system and filtering, besides the fact that in those days the knowledge level of lubrication effects in bearing life was poor and often replaced by experience. Hence, the work of Lundberg and Palmgren [18,19] was based on endurance test results with grease-lubricated bearings, like most of the related work up to the 60s, e.g. Lieblein and Zelen [20] and Tallian [21]. Therefore, the required viscosity diagram presented by Adréason and Snare [11] was also mainly based on test results produced with grease-lubricated bearings, considering only the viscosity of the base oil. Bolton [12] however, mentions some uncertainty areas in the diagram for the high and low speed areas, where there were no sufficient number of test data for complete validation. According to Bolton [12] with the knowledge of 1970s,

* Corresponding author at: SKF Engineering & Research Centre, Nieuwegein, The Netherlands.
E-mail address: guillermo.morales@skf.com (G.E. Morales-Espejel).
[1] SKF Engineering & Research Centre, Nieuwegein, The Netherlands, until May 2013.

http://dx.doi.org/10.1016/j.triboint.2014.01.023
0301-679X

Nomenclature

A	constant in the grease effective viscosity equation [s/m]
a	constant in viscosity-temperature Walther's Eq. (5) [cSt]
B	constant in Eq. (1) [m/s]
d_m	bearing mean diameter [mm]
E'	reduced Young modulus, $2/E' = (1-\nu_1^2)/E_1 + (1-\nu_2^2)/E_2$ [Pa]
E	Young modulus of the material [Pa]
f	exponent in the grease effective viscosity equation [dimensionless]
F	contact force in tribometer [N]
g	normalised activation energy, $g = E_a/R$ [1/K]
G	Dowson–Higginson dimensionless material parameter, $G = E'\alpha$ [dimensionless]
h	lubricant film thickness [m]
k	ellipticity parameter, $k = (R_y/R_x)^{2/\pi}$ [dimensionless]
n	rotating speed of the bearing in rev/min [rpm]
p_0	maximum Hertzian pressure [Pa]
R_x	reduced radius in x direction (rolling) [m]
R_y	reduced radius in y direction (transverse to rolling) [m]
R_q	r.m.s. of surface roughness combining the two surfaces [m]
$\overline{u}$	entrainment speed in the bearing [m/s]
U	Dowson–Higginson dimensionless speed parameter, $U = \overline{u}\eta_0/(E'R_x)$ [dimensionless]
T	temperature at working conditions [°C, K]
W	Dowson–Higginson dimensionless load parameter, $W = F/(E'R_x^2)$ [dimensionless]

Greek symbols

α	viscosity-pressure coefficient [Pa^{-1}]
ρ	density of lubricant [kg/m^3]
η	viscosity of the lubricant [Pa s]
η_0	dynamic viscosity of the lubricant and ambient pressure [Pa s]
Λ	lubrication quality parameter, $\Lambda = h_c/R_q$ [dimensionless]
ν	Poisson ratio [dimensionless]
ν	kinematic viscosity of the lubricant, $\nu = \eta/\rho$ [cSt]
ν_1	required or reference viscosity to obtain adequate lubrication in a bearing [cSt]
κ	lubrication quality parameter in the bearing, $\kappa = \nu/\nu_1$ [dimensionless]

Subscripts

c	central
I	minimum speed in rolling bearings considered in this paper (correspond to the left upper corner of the required viscosity diagram in ISO, Fig. 5)
II	transition speed: speed for minimum film thickness in the film thickness–speed curve for a grease lubricated contact (corresponds to the speed where the grease film thickness is parallel or equal to the base oil film thickness)
g	grease
oil	oil
eff	effective
T	at a given temperature

the required viscosity diagram area in which standard bearing life calculation procedures could be used, was in the range of $10,000 \le nd_m \le 500,000$ (in the range of $0.25 \le \overline{u} \le 12.5$ m/s). Beyond these limits, special experience and additional care would be required to safely design the application.

Currently, it is recognised that about 90% of the bearings in applications are grease lubricated [22] and it is important to understand the behaviour of grease in rolling bearings, especially in the areas of very low and very high speeds to better predict bearing life in these conditions; the present paper addresses the low speed area only. Slow rotating rolling bearings are often large-size bearings fully-flooded with grease (up to 90% of free volume) working in important applications like renewable energy, mining, marine transport, etc. Here the selection of the lubricant is critical; a proper selection methodology can contribute in considerable cost savings. Contrary, a wrong selection of the lubricant can generate huge costs and machine downtime. In these low-speed critical applications, it is often the case that engineers tend to select greases with very high base oil viscosity, since the current method requires so to ensure sufficient life in the bearing. However, these machines can operate also in speed ranges that vary from the very low to normal and they operate in a very large range of temperatures. Sometimes, the selection of very high viscosity base oils can bring unnecessary limitations in grease bleeding properties and it can generate starvation in the contacts [22]. Engineering experience also shows that greases with lower viscosity oils can properly work under very low speeds conditions and the current lubricant selection methodology does not reflect this, since the thickener effect is not considered. The detrimental effects of selecting greases with very high viscosity oils are also not considered in standard bearing life calculation methods, thus making engineers unaware of the danger. Therefore a new methodology is required that reflects the true behaviour of the grease under low speeds conditions.

It is the objective of the present paper to revisit the area of low speeds in grease lubricated fully-flooded rolling bearings and to develop a better method to account for the lubrication quality parameter κ, considering the effects of the grease thickener and not only the viscosity of the base oil. The pursued model here is of engineering type, to be used for a better selection of greases in rolling bearings.

2. Experimental work

Some researchers have measured indirectly lubricant film thickness in grease-lubricated bearings, Wilson [23] measured electrical capacitance in two designs of roller bearings (cylindrical and spherical) in the speed region of $28,500 \le nd_m \le 228,000$ (all inside the Bolton's safe zone) and concluded that grease-lubricated bearings can initially form a thicker film than the base oil but in time the film thickness is thinner than the one predicted for base oil, due to starvation and loss of oil in the grease. Muennich and Gloeckner [24] measured film thickness using electrical capacitance in roller bearings lubricated with grease, they identified transition velocities from fully flooded to starved regimes. More recently, Dong et al. [25] measured film thickness via electrical potential in the range of low speeds; they concluded that grease in this area considerable increases film thickness in comparison to the base oil alone.

Measuring film thickness in grease-lubricated bearings is not easy and the results could vary substantially depending on the

grease filling volume, initial grease distribution, grease leakage, etc. Therefore, most researchers have preferred to study grease lubrication starting with a single contact. In these conditions film thickness can be measured directly by using interferometry techniques [26–27] in a ball-on-disc tribometer. This is particularly interesting for the low-speed conditions, where the lubrication in a bearing is mainly given by grease churning mechanisms (fully-flooded lubricated bearing) rather than oil bleeding from grease, as it would happen in normal speeds. This condition can easily be maintained in a ball-on-disc tribometer, since the simulated race-way and contact is constantly being observed and because the grease can be redirected to the contact by external means, such as a scoop providing a continuous fully flooded contact.

Several researchers have measured grease film thickness in these conditions [28–31]. Yang and Qian [28] measured film thickness and proposed a model for grease lubricated contacts with the use of a "plastic" viscosity for the grease in the film thickness equation. Hargreaves and Pai [29] studied grease lubricated contacts in the range of speeds of $0.18 \leq \overline{u} \leq 0.9\ m/s$ (only the lower limit is considered outside Bolton's safe zone). They measured film thickness in grease lubricated point contacts and found that the film thickness is close or higher (between 5 and 25%) than those predicted with the base oil. In the case of "measured larger-than-predicted oil film thickness" they confirmed the results of [28] and also recommended the use the "plastic" viscosity of the grease rather than the base oil viscosity in the film thickness equation to better predict the measurements. Hurly and Cann [30] observed, at low speed, an increase in film thickness of greased contacts when decreasing the speed. More recently, Kimura et al. [31] have measured film thickness in grease lubricated contacts in the very low speed range of $0.002 \leq \overline{u} \leq 1\ m/s$; they show that in these conditions grease forms thicker films that base oil and much thicker than the predictions of Yang and Qian [28], see the schematic representation in Fig. 1. Cousseau et al. [32] measured film thickness with grease, base oil and bleed oil in the range of speed $0.1 \leq \overline{u} \leq 1\ m/s$. They found that in most of the cases the film thickness was highest for the grease followed by that of the bleed oil, whereas the base oil gave the lowest film. They proposed to use the rheological properties of the bleed oil to properly calculate the measured film thickness; in particular they suggested the use of an effective viscosity-pressure coefficient obtained from measurements.

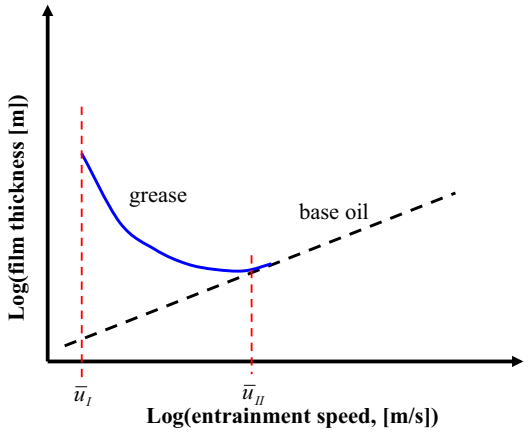

Fig. 1. Schematic representation of EHL film thickness behaviour for oil and grease in very low speeds, inspired from [30].

The experimental measurements used in this paper to derive a model are detailed and expanded in another paper by the authors [48].

2.1. Greases

As described above, slowly rotating bearings are usually fully flooded with grease to ensure sufficient lubrication. These bearings are equipped with lubrication systems that supply continuously fresh grease at defined intervals. Depending on the atmospheric temperatures and the operating conditions, these bearings experience wide temperatures, ranging between −40 °C to around 80 °C. Because slowly rotating bearings are equipped with lubrication systems and the average operating temperature is well below 80 °C, it is fair to assume that the grease that lubricate the contacts are (nearly) fresh grease. Therefore, in this study most of the measurements where done with fresh grease.

Table 1 below shows the list of commercial greases from different manufacturers that are used here. These greases cover a wide range of base oil viscosities, base oil types, thickener types and additives might be included. Some of these greases are used in slowly rotating bearing applications.

2.2. Ball-on-disc tribometer

The optical interferometry technique has been used extensively to measure film thickness of fully flooded grease lubricated single contact. The principle of this technique is widely understood and will therefore not be outlined here (see for example [30]). In this paper, lubricant film thickness measurements were performed with a Wedeven Associates Machine #5 (WAM 5) where the contact is formed between a glass disc (coated with a semi-reflective chromium layer) and a steel ball or a steel roller (see Fig. 2). To simulate and ensure fully flooded conditions, a scoop is placed at a distance before the contact to push the grease resting at the sides of the track back to the running track. Different types of fresh grease are used for the measurements (see Table 1). Speed sweep (from 10^{-4} to 0.2 m/s) film thickness measurements were carried at a maximum Hertzian contact pressure of 0.5 GPa and at different temperatures.

Fig. 3 shows an example of the results for the film thickness measurements as a function of entrainment speed at different temperatures for grease D. One can notice that the logarithmic film thickness as a function of logarithmic entrainment speed formed "V" shape curves for fully flooded grease lubricated

Table 1
List the basic properties of greases used in this paper.

Grease	Thickener type	Oil type	ν, @ 40 °C [cSt] (base oil)	ν, @ 100 °C [cSt] (base oil)
A	Lithium complex	Synthetic/PAO	191	30
B	Lithium complex	Mineral/PAO	280	22
C	Lithium complex	Polyglycol/PAO	375	50
D	Lithium	Mineral	98	9.4
E	Lithium	Mineral	200	18
F	Complex calcium sulphonate	Mineral and synthetic	80	8.6
G	Diurea	Mineral	115	12.2

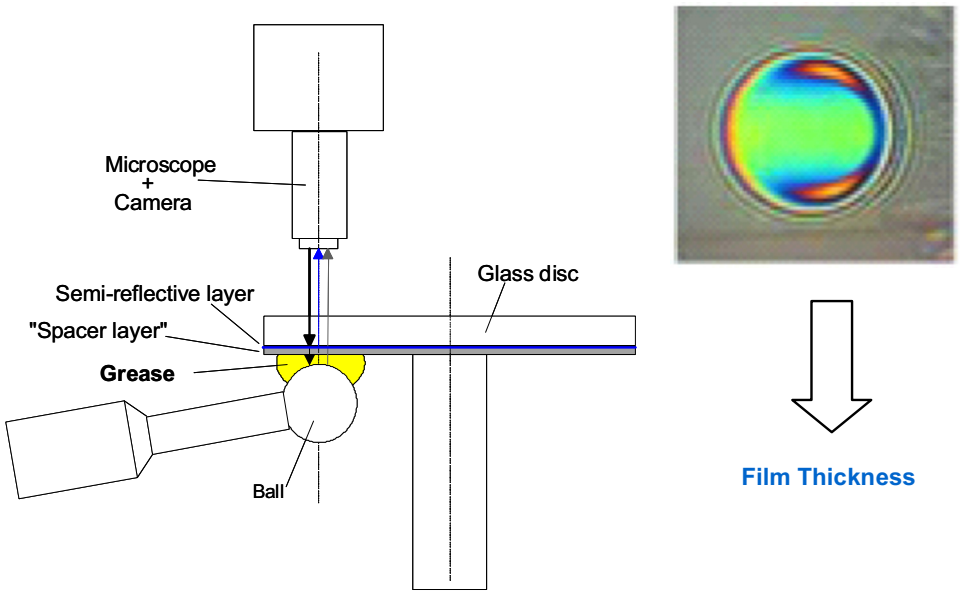

Fig. 2. Schematic representation of film thickness measurements using interferrometry technique.

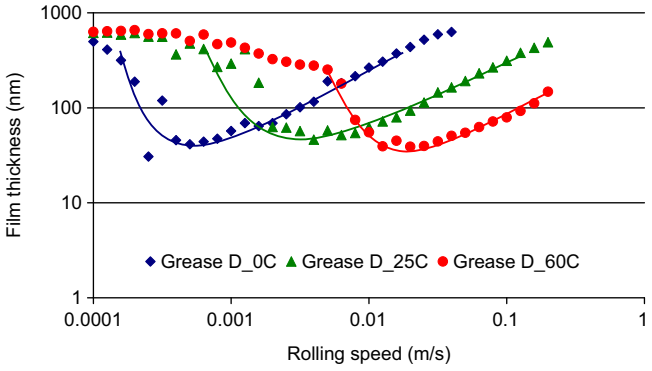

Fig. 3. An example of film thickness measurements results as a function of entrainment speed at different temperatures.

contacts as opposed to a straight line for fully flooded oil lubricated contacts. This behaviour will be further discussed and modelled here.

The range of test conditions in the WAM is summarised in Table 2.

2.3. Capacitance measurements in full-bearings

As shown in Fig. 3, at low entrainment speeds, fully-flooded grease lubricated single contact revealed the existence of relatively thick EHL lubricating film. To demonstrate that this behaviour is also observed in bearings, the electrical capacitance method is chosen to measure film thickness of a fully flooded grease lubricated deep groove ball bearing (see Fig. 4). When two bodies in contact are separated by thin film lubricating layer, the measured capacitance can be correlated to EHL film thickness using the following equation:

$$C = \varepsilon_0 \varepsilon_r (A/h) \quad (1)$$

where C is the measured capacitance, A is the area (which is assumed to be the Hertzian contact area) separated by a dielectric material with dielectric constant, h is the related film thickness, ε_r is dielectric constant (relative permittivity) and ε_0 is the dielectric constant of vacuum. Ideally, for constant operating conditions, the values of ε_0, ε_r, and A are constant, therefore, the measured values of capacitance are inversely proportional to the EHL film thickness.

Recently, Jablonka et al. [33] showed the good agreement between film thickness measurements obtained from the electrical capacitance method and optical interferrometry technique over a range of film thickness. Further, Jablonka et al. [34] made comparative measurements of EHD Film thickness in a ball-on-flat rig and a rolling bearing. This was realized by applying the electrical capacitance method on a modified ball bearing 6306 ETN9/C3. This bearing has 7 steel balls. Six steel balls are replaced with 6 ceramic (silicon nitride) balls (with the same diameter of that of the steel ball); therefore only one steel ball remains (see Fig. 4). Since silicon nitrate balls are non-conductive, the measured value of the capacitance corresponds to the film thickness between the steel balls and the rings. An external trigger is used to start the data acquisition when the steel ball is entering and exiting the loaded zone. With this method, qualitative film thickness measurement in a bearing can be realized. A radial load of 1 kN (~1.34 GPa maximum Hertzian contact pressure on the steel ball) is applied to the bearing. The surface speed of the inner ring is varied between 1 and 6 mm/s at low speed region and between 0.2 and 1.6 m/s at high speed region. The operating conditions used in the experiments are summarised in Table 3.

First the rig was calibrated using measurements with oil of the same viscosity as the grease base oil at the two test temperatures 60 °C and 100 °C. Plots of Lubcheck-voltage versus speed were obtained. These plots were converted into Lubcheck-voltage versus film thickness calibration curve by assuming that the oils develop films that can be predicted by using the Hamrock and Dowson film thickness formula. Next, the measurements with grease were done and the Lubcheck-voltage could be translated into film thickness by using this calibration relation again.

The bearing was fully packed with fresh grease (see Fig. 5). Transparent shields were used to retain as much as possible grease inside the bearing. A heating gun was used to enable the experiment at elevated temperatures (in this case 60 °C and 100 °C). The measurement results (see Fig. 6) show qualitatively that thick EHL film thickness not only exists in ball-on-disc experiments but also

Table 2
Ball on disc rig range of test conditions.

Test conditions	Load (N)	P_{max} (GPa)	Geometry	R_q, roughness (nm)	Temperature (°C)	Speed range (m/s)
With ball	20 ± 2	0.46	$R_x = R_y = 10.32$ mm	< 10	0, 10, 25, 40, 60	10^{-4}–0.2
With roller	20 ± 2	0.77	$R_x = 5.3$ mm; $R_y = 4.2$ mm	< 10	25	10^{-4}–0.2

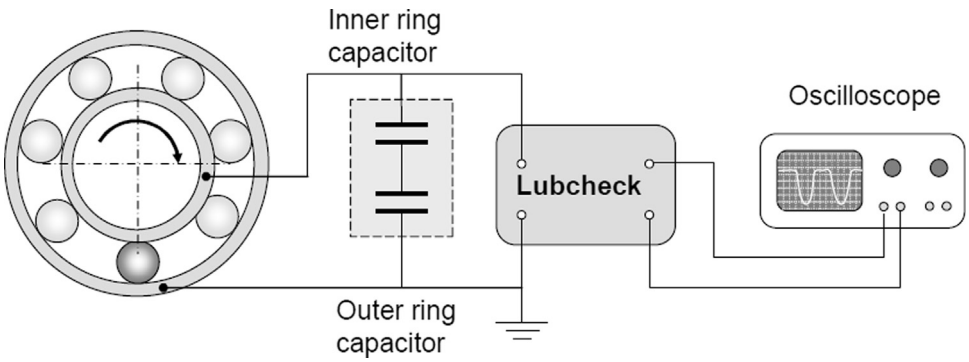

Fig. 4. Schematic representation of film thickness measurement using capacitance method [34].

Table 3
Full bearing test conditions with DGBB 6306 ETN9/C3.

Radial load (N)	Maximum load in contact (N)	P_{max} (GPa)	Temperature (°C)	Speed range (RPM)	Speed range (m/s)
1000	606	1.34	60,100	1–5 RPM and 160–1280 RPM	1.23×10^{-3}–6.15×10^{-3} and 1.91×10^{-1}–1.57

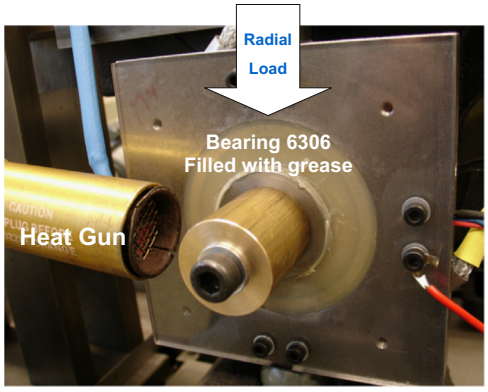

Fig. 5. Experimental setup showing fully flooded grease lubricated 6306 bearing.

exists in bearings operating at low speed conditions, as observed in grease lubricated single contact described earlier.

2.4. Transition speed U_{II} as a function of temperature

By performing ball-on-disc film thickness measurements with commercial lithium grease in the starved regime, Cann [35] showed that the grease film thickness consists of a fraction formed by hydrodynamic effects and by a residual or boundary layer:

$$h = h_R + h_{EHL} \tag{2}$$

The residual film thickness varied between $6 < h_R < 80$ nm. She showed that the layers are clearly thicker at higher temperatures. Similar boundary layers were found by Cann and Spikes [36] on polymer solutions and by Smeeth et al. [37] for a large number of polymer solutions (VI improvers). Also in [37] it was found that the boundary film formation was more evident as the temperature

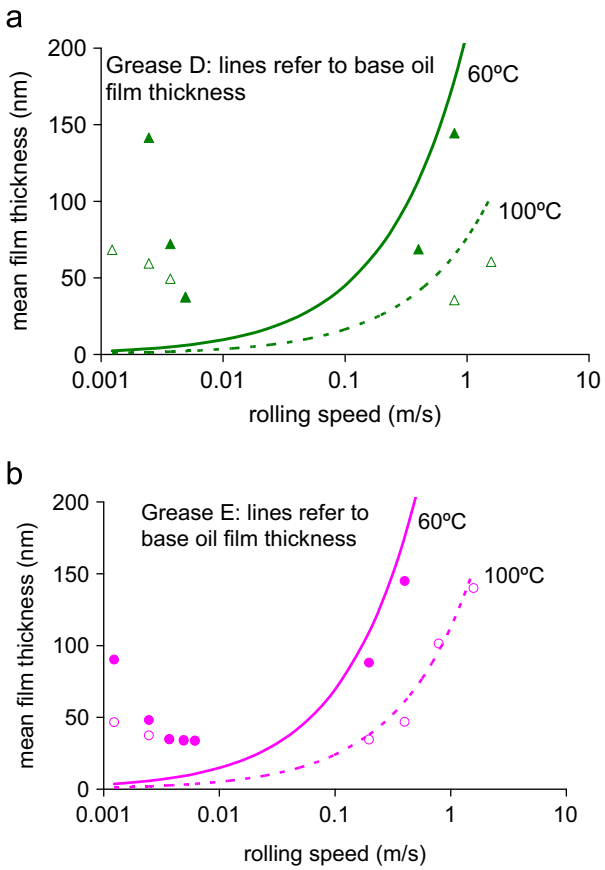

Fig. 6. Qualitative measurement results of film thickness in a modified 6206 rolling bearing with two greases. Closed symbols: 60 °C; Open symbols: 100 °C. (a) Grease D and (b) Grease E.

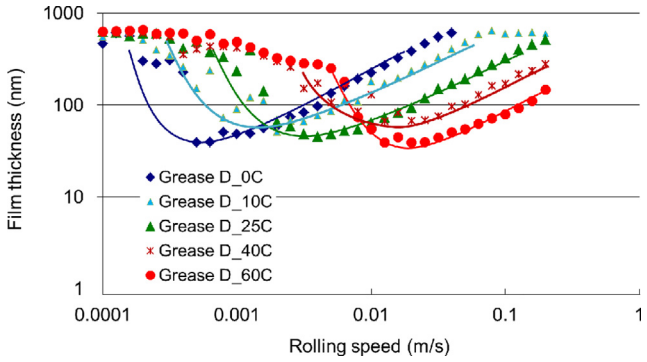

Fig. 7. Film thickness measurements for grease D.

Table 4
Values for the parameter g from Eq. (3) for different greases as described in Table 1.

Grease (Table 1)	D	E	G	F
g	0.0585	0.0787	0.0203	0.0807

is raised. In these publications it is proposed that these boundary layers follow an adsorption mechanism and contribute in the film thickness formation. However, in a more recent publication Lubrecht et al. [50] suggest that the grease thickener is initially entrapped by pure mechanical process. This mechanism can, of course, also contribute in the film formation.

At this point, regardless of the mechanisms forming the observed thicker film, the thickness of the boundary layer is reflected in the speed at which the film thickness–speed curve no longer follows the traditional EHL behaviour, denoted by $\overline{u}_{II}$ in Fig. 1. From the experiments, it has been observed that the location of this point varies with temperature in an exponential form:

$$\overline{u}_{II} = B\exp(gT), \tag{3}$$

where for most of the cases tested $B \approx 0.0005$ [m/s]. Fig. 7 shows an example of the film thickness measurement on the WAM5, where the increase of the minimum speed $\overline{u}_{II}$ with temperature is clearly visible.

Film thicknesses measured as shown in Fig. 7 have also been carried out for the other greases. The minimum speed $\overline{u}_{II}$ has been fitted to Eq. (3) giving the results of Table 4.

3. Film thickness model description

Several authors have developed models for the estimation of film thickness in grease lubricated EHL contacts. Kauzlarich and Greenwood [38] assumed Herschel–Bulkley rheology for the grease and with the use of a Grubin-type model were able to calculate film thickness in grease-lubricated EHL contacts. Jonkisz and Krzeminski-Freda [39] extended the analysis to the complete pressure and film thickness distributions. They concluded that grease gives very similar film thickness and pressures as oil, with only some local differences. Dong and Qian [40] used a more sophisticated Bauer rheology model and solved the EHL grease-lubricated line contact numerically, predicting slightly higher film thickness values for grease than for oil. Bordenet et al. [41] utilise also a Bauer rheology model and solve the point contact problem numerically, obtaining similar conclusions as Dong and Qian [40].

All the models discussed above somehow state that the yield stress of the grease has almost no effect in the film thickness behaviour. The models have also been used in speed ranges in general higher than the interest in the present paper. Currently, to the knowledge of the authors, only [31] attempts to model the very

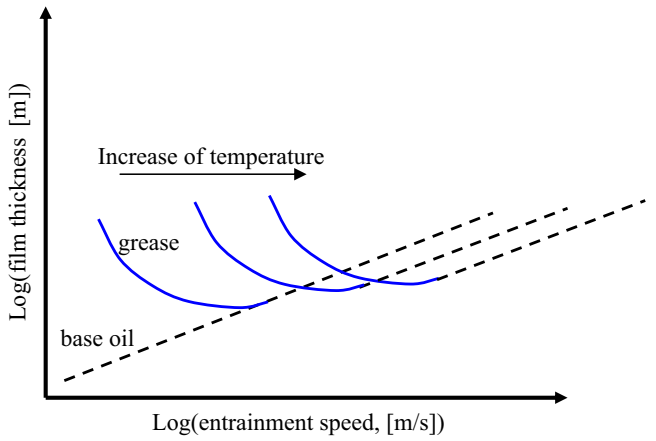

Fig. 8. Schematic representation of EHL film thickness behaviour for oil and grease in very low speeds, as affected by temperature increase.

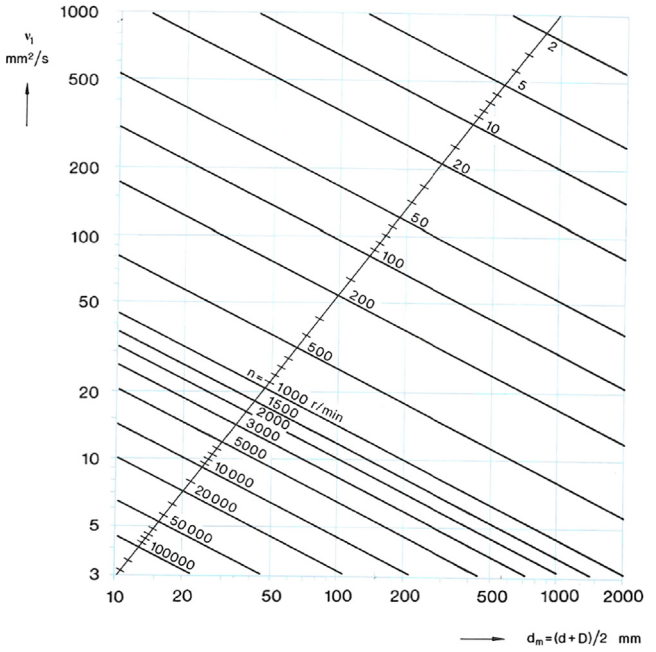

Fig. 9. Required viscosity diagram for rolling bearings as given by ISO 281 [15].

low speed area by using a Carreau-Yasuda non-Newtonian model with an apparent viscosity that increases at low speed due to the effect of the thickener. They introduce a time-dependent correction in the shear rate from the oscillation in the rheometer and are able to predict the "V" shape observed in film thickness measurements at very low speed, schematically represented in Fig. 1.

Experiments in the authors' laboratory which will be shown in Fig. 11, show that the V-shape moves to higher speeds at higher temperatures (see Fig. 8). In the current section a model able to capture this behaviour is discussed.

As suggested previously [29,32] here the idea of using equivalent rheological properties for the grease in order to approximate better the film thickness in an EHL contact is retained. In particular the low speed area is of interest, i.e. $250 \le nd_m \le 10,000$ (i.e. $0.0063 \le \overline{u} \le 0.25\ m/s$). The lower speed limit is obtained from the lowest speed that can be read in the required viscosity diagram of ISO 281 [15] (left upper corner, here taken as $nd_m = 250$), see Fig. 9. The higher limit corresponds to the lower limit of speed for Bolton's safe zone, for higher speeds, it is found that the use of base oil viscosity is safe.

Here an effective viscosity of the grease as a function of speed and temperature will be calculated and used in standard EHL film

thickness formulae for the safe calculation of film thickness in grease lubricated contacts.

3.1. Estimation of effective viscosity of the grease from film thickness measurements

From the film thickness measurements in fully flooded conditions and low rolling speed experiments carried out in this study using both a ball-on-disc (and roller-on-disc) and also a full bearing, it is clear that grease lubrication follows a different trend with speed in relation to oil lubrication. Grease provides greater film thickness at very low speeds up to a certain limit ($\overline{u}_I$), but as the speed increases the film-thickness curve eventually joins or follows the one of the base oil (Fig. 1). The behaviour of the grease in the low-speed zone is equivalent to having grease with an effective viscosity which is high at very low speeds but it tends towards the base oil viscosity as the speed increases ($\overline{u}_{II}$).

Therefore, here the effective dynamic viscosity of the grease ($\eta_{g.eff}$) is defined as the grease viscosity needed in a standard oil EHL film thickness formulae to calculate the measured film thickness in an experiment.

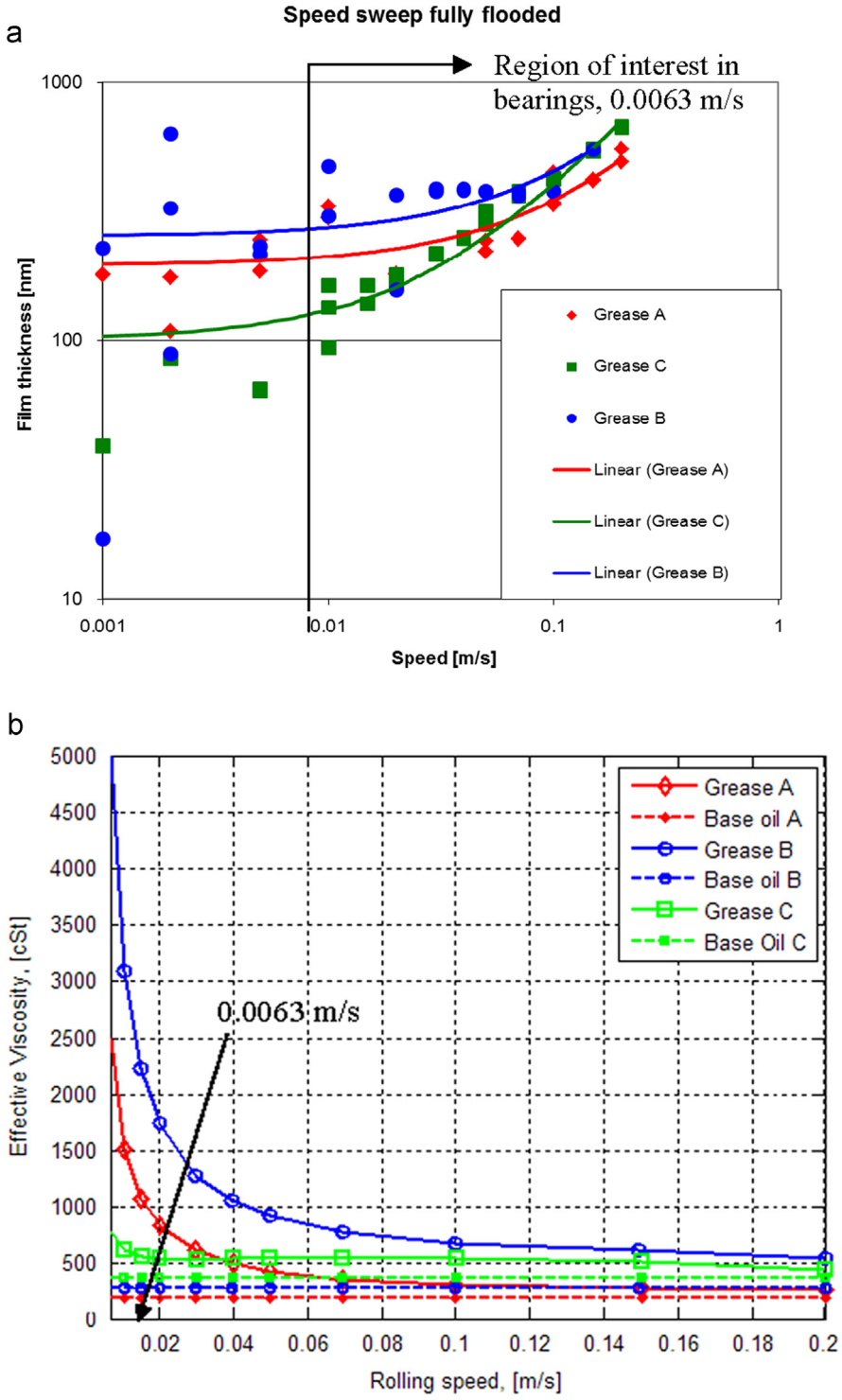

Fig. 10. (a) Measured film thickness (including trend lines) and (b) calculated kinematic viscosity of the three greases of Table 5.

Table 5
Operating conditions and lubricant data in the ball-on-disc tribometer for the example of effective viscosity for three lithium complex greases. Test done at 40 °C.

Grease	F, [N]	Ball diameter, [mm]	E', [GPa]	ν, @ 40 °C [cSt] (base oil)	ν, @ 100 °C [cSt] (base oil)	α, [GPa^{-1}] @ 40 °C	p_0, [GPa]
A	20	20.6	102.19	191	30	40	0.456
B	20	20.6	102.19	280	22	30	0.456
C	20	20.6	102.19	375	50	35	0.456

Note: α values are obtained from the grease highest speed film thickness measurements at each temperature (nearly base oil behaviour).

Hence, a common EHL central film thickness formula for oil is picked-up e.g. Hamrock and Dowson [42], which can be written as

$$h_c = 2.69R_x(1-0.61e^{-0.73k})G^{0.53}U^{0.67}W^{-0.067} \tag{4}$$

with G, U and W being the Dowson and Higginson dimensionless variables, where $G=E'\alpha$, $W=F/(E'R_x^2)$. For a known film thickness h_c, the viscosity η_0 can be found in $U=\overline{u}\eta_0/(E'R_x)$, with $\overline{u}$ is the new speed, R_x is the reduced radius in the x-direction (rolling). Hence, Eq. (4) can be solved for η_0 at every speed $\overline{u}$ value. In grease lubrication this viscosity represents the effective viscosity of the grease $\eta_{g.eff}$.

Fig. 10 shows an example of a measured film thickness in a grease-lubricated experiment, using a ball-on-disc tribometer with the operating conditions from Table 5. Fig. 10(a) shows the film thickness measurements with variable speed (including trend lines) and Fig. 10(b) shows the corresponding effective viscosity of the grease as obtained after solving Eq. (4) for film thickness values taken at points on the trend lines.

3.2. Calculation of effective viscosity as a function of speed

It was discussed above that the effective viscosity of the grease varies with the entrainment speed, following the schematics of Fig. 1. A model simple enough that can describe this behaviour is given by the following equation:

$$\eta_{g.eff} = \eta_{0.oil}\left[\coth(A\overline{u})\right]^f \tag{5}$$

Notice that according to Eq. (5), $\eta_{g.eff}\to\eta_{0.oil}$ for $\overline{u}\to\infty$, $\forall\, f\neq 0$ and that this is a convenient behaviour since at higher speeds (or higher shear rates) grease tends to behave as its base oil. Notice also that $\eta_{g.eff}\to\infty$, for $\overline{u}\to 0$. However, this is avoided by using this equation only for $\overline{u}>0.0063\ m/s$.

Eq. (5) has two constants that can be obtained by applying a collocation method with the use of two points in speed of a measured viscosity curve. The two convenient points are $\overline{u}_I=0.0063\ m/s$ (the lowest speed that can be read in the required viscosity diagram of ISO [15], here taken as $nd_m=250$) and $\overline{u}_{II}=$ speed for which the effective viscosity can be considered equal or parallel to the base oil viscosity (normally it corresponds to the dip in the curve of Fig. 1).

Therefore, taking the two collocation points:

$$\begin{aligned}\eta_{g.eff_I} &= \eta_{0.oil}\left[\coth(A\overline{u}_I)\right]^f\\ \eta_{g.eff_{II}} &= \eta_{0.oil}\left[\coth(A\overline{u}_{II})\right]^f\end{aligned} \tag{6}$$

Eq. (6) can be solved for A and f by a simple iterative scheme. Alternatively, the approximated analytical solution described in Appendix A can be applied.

3.3. Effect of temperature

It has been found that the calculated effective viscosity of the grease can be interpolated to any temperature also by using Walther's equation for oil kinematic viscosity [43],

$$\nu_{T,cSt} = 10^{\left[K_W - C\log_{10}(T)\right]} - a \tag{7}$$

with,

$$\begin{aligned}K_W &= \log_{10}[\log_{10}(\nu_{T_1,cSt}+a)]+C\log_{10}(T_1)\\ C &= \{\log_{10}[\log_{10}(\nu_{T_1,cSt}+a)]\\ &\quad -\log_{10}[\log_{10}(\nu_{T_2,cSt}+a)]\}/[\log_{10}(T_2)-\log_{10}(T_1)]\\ a &= 0.8\end{aligned} \tag{8}$$

and all temperatures in [K].

To convert between grease dynamic and kinematic effective viscosities, the same relationship as for oil shows to be effective,

$$\nu_{g.eff,cSt} = \eta_{g.eff}/[(\rho_{oil})(1\times 10^{-6})] \tag{9}$$

with ν in [cSt], η in [Pas] and $\rho_{oil}=980\ \mathrm{kg/m^3}$.

Eqs. (7) and (9) have been verified with around 8 different greases (same greases as in Section 2) in a temperature range between 0 and 80 °C.

3.4. Film thickness calculation and verification process

Characterisation of greases involves the following steps:

1. Film thickness measurements in a ball-on-disc tribometer at least for two speeds $\overline{u}_I$ and $\overline{u}_{II}$ at two different temperatures.
2. If the point $\overline{u}_{II}$ is unknown, the whole speed sweep is needed, until the same behaviour as base oil is found.
3. With the use of Eq. (5) the whole curve $\eta_{g.eff}$ vs. $\overline{u}$ for the two temperatures can be reconstructed.
4. With the use of Eqs. (7) and (8) curves for any other temperature can be approximated.
5. According to the schematics of Fig. 8, an increase in temperature displaces the location of point $\overline{u}_{II}$ towards a higher velocity. This point can be calculated with eq. (3). If the constants (B,g) for this equation are unknown, the grease needs to be characterised at different temperatures.
6. Given any $\eta_{g.eff}$ vs. $\overline{u}$ curve, a film thickness curve h_c vs. $\overline{u}$ can be calculated by using Eq. (4).
7. This calculated curve can be compared with the measured curve to check the accuracy of the whole procedure.

3.5. Validation of the model

Film thickness predictions with the model have been compared with measurements at different temperatures. The results are summarised in this section. Note that when the curve dip ($\overline{u}_{II}$) is located before the applicability limit ($\overline{u}_I$), the model will simply predict $\eta_{g.eff}=\eta_{0.oil}$. Fig. 11 shows a comparison of the calculated and measured film thickness for a grease lubricated ball-on-disc tribometer with operating conditions as given in Table 6. The properties of the used greases are summarised in Table 7.

Notice that in Table 7, the viscosity-pressure coefficient (α) values were not measured directly, but rather they were calculated from the grease film thickness measurements in the high speed

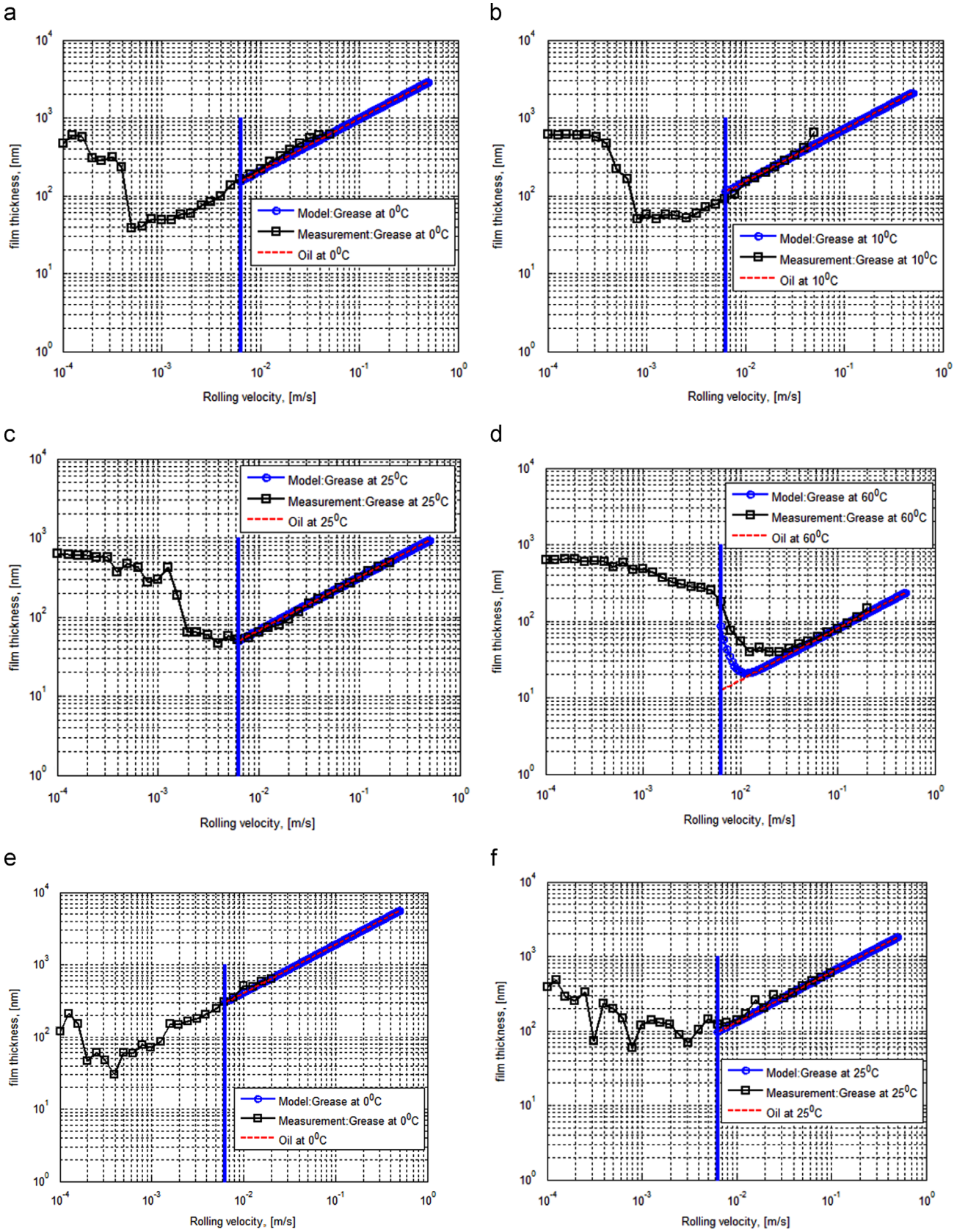

Fig. 11. Comparison of central film thickness measurements vs. calculations for ball-on-disc experiments with operating conditions given in Table 6 and four greases as described in Table 7 at different temperatures. (a) Grease D, 0 °C, (b) Grease D, 10 °C, (c) Grease D, 25 °C, (d) Grease D, 60 °C, (e) Grease E, 0 °C, (f) Grease E, 25 °C, (g) Grease E, 40 °C, (h) Grease E, 60 °C, (i) Grease F, 0 °C, (j) Grease F, 25 °C, (k) Grease F, 40 °C, (l) Grease F, 60 °C, (m) Grease G, 0 °C, and (n) Grease G, 60 °C.

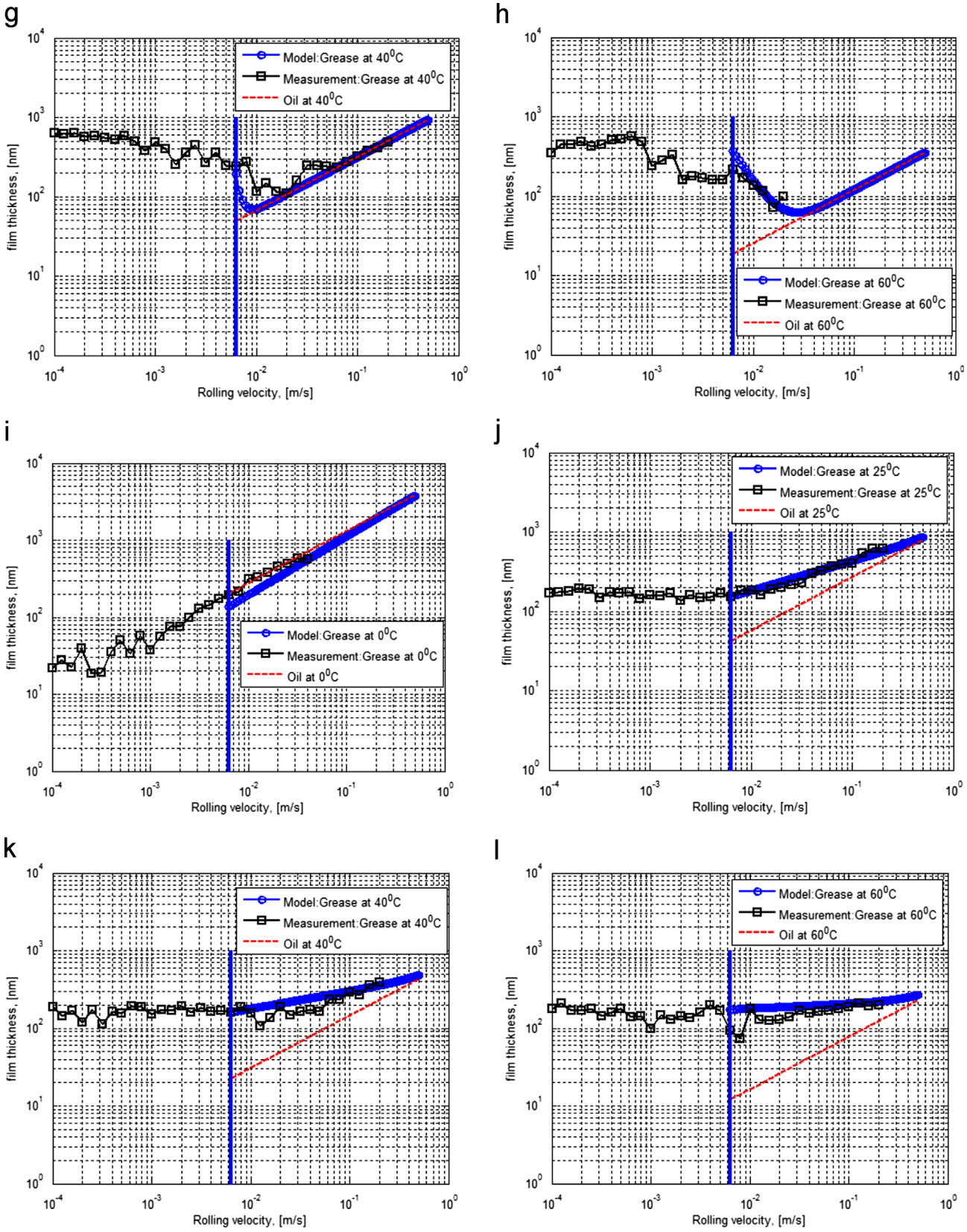

Fig. 11. (*continued*)

end, where the film thickness is only slightly higher than the thickness determined by the base oil. In Table 7, α values appear somehow larger than those of the usual oil values.

In general the model predicts the film thickness well. For grease D the dip in the curve is usually located before $\overline{u}_l$, thus the model predicts $h_c = h_{c.oil}$, except for the case of 60 °C (Fig. 11(d)) in which

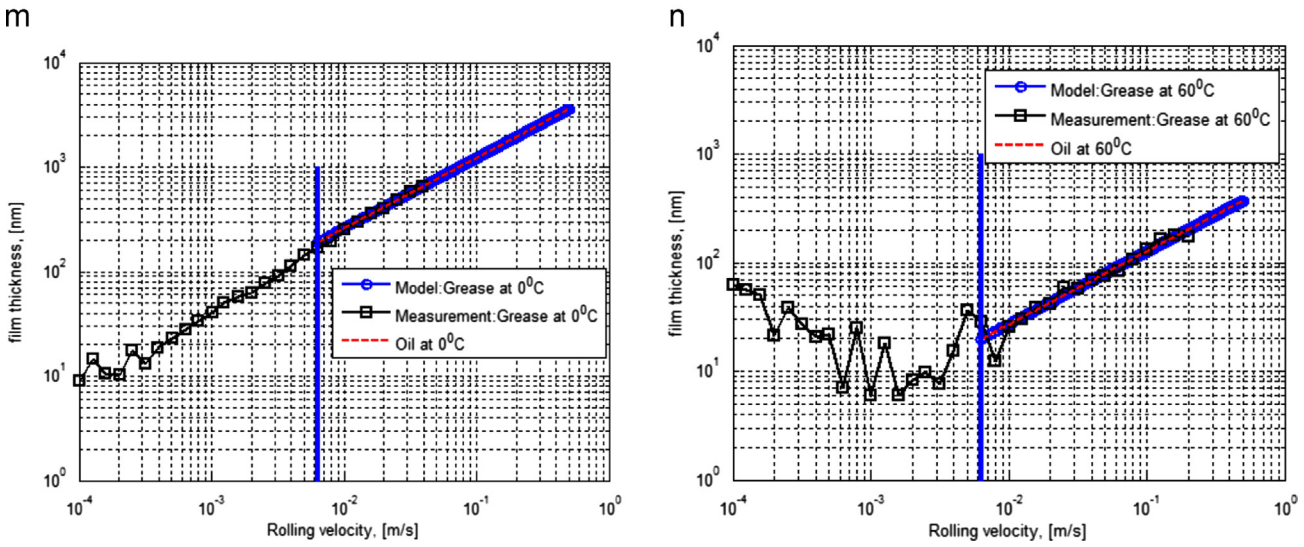

Fig. 11. (*continued*)

the film thickness is reduced with increasing speed until it joins the oil film thickness curve, the model follows well the same trend. Grease E has a behaviour that is slightly more affected by temperature since the dip speed is higher than $\overline{u}_l$, already at 40 °C (Fig. 11 (g) and (h)). Grease F has a different behaviour than the other greases: it does not exhibit a very marked dip in the curves (except at 0 °C) but rather a constant value of film thickness at very low speeds and gradually becoming parallel to the oil film thickness. In any case, the model shows good agreement for this grease too.

Finally, grease F shows the dip at speeds lower than $\overline{u}_l$, even at 60 °C (Fig. 11(n)). In all cases the model predicts the behaviour of the oil quite well.

3.6. Grease ageing effect

Already in the 1950s it was recognised that the thickener material in grease changes its properties under shear as experienced in a rolling bearing. This was studied in full bearings but also in laboratory equipment such as in the roll stability test (ASTM D1831), Renshaw [44], Bondi et al. [45,46]. For soap greases the ratio of length and diameter changes reducing the consistency of the grease. This also has an impact on the film thickness as shown by Poon [47], who measured film thickness in a disk machine using a magnetic reluctance technique.

The degradation will be a function of time and shear rate. It may be assumed that the grease degradation will not be too severe in bearings that are operating at extremely low speed. These are usually fully packed with grease and the relative volume passing the contacts will be relatively low. The measurements that were shown here were done on fresh grease. However, the model can account for grease ageing if the parameters of Eq. (6) are calculated using measurements with aged grease. The behaviour of aged grease will tend to be different, see [51].

3.7. Point vs. line contact

In the WAM tribometer, the ball was also replaced by a spherical roller in order to produce an elongated elliptical contact and some film thickness measurements where repeated. The results matched very well the ball-on-disc, showing that the observed behaviour represents both point and line contacts.

4. Rolling bearing application example for the model

The required viscosity (ν_1[cSt]) for a bearing can be calculated by using the diagram from ISO 281 [15] (Fig. 4) or related equations. In an oil lubricated bearing the lubrication quality factor κ is then calculated from the ratio of the actual used viscosity (ν, [cSt]) and this ν_1. Traditionally, in grease-lubricated bearings the actual viscosity ν is calculated by using the viscosity of the base oil (ν_{oil}) disregarding completely the contribution of the thickener which is apparent at very low speeds. In this section, calculation examples with bearings will be shown where the traditional method of using ν_{oil} is compared with the present method of rather using the effective viscosity for the grease $\nu_{g.eff}$, as defined by Eqs. (5)–(9).

The example data is given in Table 8, required viscosities are calculated from the diagram of Fig. 9 and actual viscosities are calculated using Eqs. (5)–(9). The results for κ and the bearing life are summarised in Table 9.

From the results of Table 9 it can be seen that in all cases when the velocity is very low, the current model predicts higher viscosities than the base oil viscosity, which is in better agreement with film thickness measurements and with engineers' experience. This represents in general higher predicted bearing lives, because the grease thickener lubricating properties and the effect of the bled oil are also considered in the proposed calculation method.

5. Discussion and conclusions

Film thickness measurements at low velocity with grease of fully-flooded contacts were presented using different greases and different operating conditions. In general the measurements show thicker film thicknesses than the predictions using base oil. This situation represents the behaviour of fully-flooded slow rotating grease lubricated bearings. The experiments show that the use of the base-oil viscosity for the calculation of the lubrication conditions of the bearing is not always safe. An empirical model has been proposed, based on the measurements presented here that can be used to calculate the effective viscosity of the grease in those conditions. The model shows good agreement with the ball-on-disc interferometry measurements and also with bearing measurements carried out using an electrical capacitance method. The understanding of the film formation mechanisms of grease in

Table 6
Operating conditions in the ball-on-disc tribometer.

F, [N]	Ball diameter, [mm]	E', [GPa]	p_0, [GPa]	T, [°C]	$\overline{u}$, [m/s]
20	20.6	102.19	0.456	Variable	variable

Table 7
Properties of the greases used in the ball-on-disc film thickness measurements.

Grease	Thickener type	Oil type	ν, @ 40 °C [cSt] (base oil)	ν, @ 100 °C [cSt] (base oil)	α, [GPa^{-1}] @ 10 °C
D	Lithium	Mineral	98	9.4	40
E	Lithium	Mineral	200	18	33
F	Complex calcium sulphonate	Mineral and synthetic	80	8.6	45
G	Diurea	Mineral	115	12.2	37

Note: α values are obtained from the grease highest speed film thickness measurements where the viscosity approximates that of the base-oil.

Table 8
Example cases for lubrication quality calculation in rolling bearings.

Example	d_m, [mm]	n, [rpm]	Operating T, [°C]	Grease identifier
1	1000	0.3	60	D
2	1000	5	10	D
3	500	10	40	E
4	500	0.8	60	E
5	500	1	60	F

Table 9
Results of example cases for lubrication quality calculation and life in rolling bearings.

Example	$\overline{u}$, [m/s]	$\nu_{g.eff}$, [cSt]	ν_{oil}, [cSt]	ν_1, [cSt]	κ_g	κ_{oil}	$L_{10.g}/L_{10.oil}$ (radial roller bearing) with $e_cC_u/P=1$
1	0.0075	250	37.7	3881	0.064	0.0097	~1
2	0.125	37.7	37.7	372	0.01	0.01	1
3	0.125	200	200	295	0.678	0.678	1
4	0.01	1036	73	2423	0.427	0.03	~5
5	0.0125	900	31	2012	0.447	0.015	~8

Note: for life calculations, $\kappa<0.1$ is taken as $\kappa=0.1$ (minimum value in ISO 281).

the above conditions needs further explanation, and will remain as an important objective for the authors in future research. However, the existent hypotheses available in the literature have been mentioned in the paper. Besides, it should be noted that commercial greases might contain film-forming additives and polymers which can substantially contribute in this aspect. This, of course, has not been discussed in-depth in the current article.

Therefore the following conclusions can be drawn:

1. In fully-flooded, low speed situations, grease can exhibit substantially thicker film thickness respect to its base oil. As the speed increases, the film thickness tends towards the base-oil predictions. The use of the base-oil properties for the calculation of film thickness is these conditions can show large discrepancy versus the measurements. Therefore a new method is needed.
2. The concept of effective viscosity of the grease as a way to reproduce the film thickness measurements is an effective way to better estimate the lubrication conditions in fully-flooded slowly-rotating bearings, as shown by the bearing film thickness measurements.
3. The proposed method can characterise a new grease with only a few film thickness measurements, making it realistic and simple to use.

Aknowledgment

The authors wish to thank Mr. Alexander de Vries Director SKF Group Product Development, for his permission to publish this article. The authors also wish to thank Mr. R. Meeuwenoord and Mr. Storken for providing them with some of the measurements presented here and Dr. J.H.H. Bongaerts for the discussions on the capacitance method.

Appendix A. Analytical approximation to the grease effective viscosity

From Eq. (6):

$$(1/\overline{u}_I)\coth^{-1}[(\eta_{g.eff_I}/\eta_{0.oil})^{1/f}]=A$$
$$(1/\overline{u}_{II})\coth^{-1}[(\eta_{g.eff_{II}}/\eta_{0.oil})^{1/f}]=A \quad \text{(A1)}$$

Thus, equating Eq. (A1) leads:

$$(1/\overline{u}_I)\coth^{-1}[(\eta_{g.eff_I}/\eta_{0.oil})^{1/f}]=(1/\overline{u}_{II})\coth^{-1}[(\eta_{g.eff_{II}}/\eta_{0.oil})^{1/f}] \quad \text{(A2)}$$

Notice that in general $\eta_{g.eff_{II}} \approx \eta_{0.oil}$, so $\coth^{-1}[(\eta_{g.eff_{II}}/\eta_{0.oil})^{1/f}] \approx \infty$. Take a large constant $K = \coth^{-1}[(\eta_{g.eff_{II}}/\eta_{0.oil})^{1/f}]$, therefore Eq. (A2) can be rewritten as

$$(1/\overline{u}_I)\coth^{-1}[(\eta_{g.eff_I}/\eta_{0.oil})^{1/f}] \approx K/\overline{u}_{II} \tag{A3}$$

From which f can be solved,

$$f \approx \frac{Ln(\eta_{g.eff_I}/\eta_{0.oil})}{Ln[\coth(K\overline{u}_I/\overline{u}_{II})]} \tag{A4}$$

and A can be obtained from any of Eq (A1).

Typical values of K with good results are of around $K \geq 5$.

References

[1] von Mohrenstein-Ertel A. Die Berechnung der Hydrodynamischen Schmierung Gekrümmter Oberflächen unter Hoher Belastung und Relativbewegung, Fortschrittsberichte VDI, Ser. 1 No. 115, Lang, OR, Oster, P, editors. VDI Verlag: Düsseldorf, 1949. First Published in 1945 in Russian under the name A.M. Ertel.

[2] Grubin AN, Investigation of the contact of machine components. Central Scientific Research Institute for Technology and Mechanical Engineering: Moscow, DSIR translation no. 337; 1949.

[3] Tallian TE, Chiu YP, Huttenlocher DF, Kamenshine JA, Sibley LB, Sindlinger NE. Lubricant films in rolling contact of rough surfaces. ASLE Trans 1964;**7**:109–26.

[4] Tallian TE. Pressure and traction rippling in elastohydrodynamic contact and rough surfaces. Trans ASME: J Tribol 1974;119:398–409.

[5] Liu JY, Tallian TE, McCool JI. Dependence of bearing fatigue life on film thickness to surface roughness ratio. ASLE Trans 1975;18:144–52.

[6] Tallian TE, Chiu YP, van Amerongen E. Prediction of traction and microgeometry effects on rolling contact fatigue life. Trans ASME: J Tribol 1978;100:156–66.

[7] Skurka J. Elastohydrodynamic lubrication of roller bearings. Trans ASME: J Lubr Tech 1970;92(2):281–91.

[8] Danner CH. Fatigue life of tapered roller bearings under minimum lubricant film. ASLE Trans 1970;13(4):241–50.

[9] SKF General Catalogue 2800 E/GB 600; 1970.

[10] Bamberg EN, editor. ASME Engineering Design Guide; 1971.

[11] Andréason S, Snare B. Adjusted rating life of rolling bearings. Ball Bear J 1975;184:1–6.

[12] Bolton WK. Elastohydrodynamic in practice, rolling contact fatigue: performance testing of lubricants. In: Tourret R, Wright EP, editors. The Institute of Pretroleum, London; 1977. p. 17–25.

[13] Heemskerk R. EHD lubrication in rolling bearings – review of theory and influence of fatigue life. Stratto Tribol Lubrif 1980;4:3–7.

[14] Ioannides E, Bergling G, Gabelli A. An analytical formulation for the life of rolling bearings. Acta Polytech Scand Mech Eng Ser 1999;137.

[15] International Standard. Rolling bearings – dynamic load rating and rating life. ISO 281; 2007.

[16] Gabelli A, Morales-Espejel GE, Ioannides E. Particle damage in hertzian contacts and life ratings in rolling bearings. STLE Tribol Trans 2008;51:428–45.

[17] Morales-Espejel GE, Gabelli A, Ioannides E. Micro-geometry lubrication and life ratings of rolling bearings. Proc Inst. Mech Eng C, J Mech Eng Sci 2010;224:2610–26.

[18] Lundberg G, Palmgren A. Dynamic capacity of rolling bearings. Acta Polytech, Mech Eng Ser 1947;1(3):1–52.

[19] Lundberg G, Palmgren A. Dynamic capacity of roller bearings. Acta Polytech, Mech Eng Ser 1952;2(4):96–127.

[20] Lieblein J, Zelen M. Statistical investigation of the fatigue life of deep-groove ball bearings. J Res Natl Bureau Stand 1956;57(5):273–316 (Research Paper 2719).

[21] Tallian TE. Weibull distribution of rolling contact fatigue life and deviations therefrom. ASLE Trans 1962;5(1):183–96.

[22] Lugt PM. Grease lubrication in rolling bearings. John Wiley & Sons, Ltd.; 2013 (Tribology series).

[23] Wilson AR. The relative thickness of grease and oil films in rolling bearings. Proc Inst Mech Eng 1979;193:185–92.

[24] Muennich HC, Gloeckner HJR. Elastohydrodynamic lubrication of grease-lubricated rolling bearings. ASLE Trans 1980;23(1):45–52.

[25] Dong D, KomoriyaT, Endo T, Kimura Y. Monitoring lubrication conditions with grease in ball bearings, paper B2-10. In: Proceedings of the international tribology conference, Hiroshima 2011, Hiroshima, Japan.

[26] Gohar R, Cameron A. Optical measurement of oil film thickness under elastohydrodynamic lubrication. Nature 1963;200:458.

[27] Gohar R, Cameron A. The mapping of elastohydrodynamic contacts. ASLE Trans 1967;10:215–25.

[28] Yang Z, Qian X. A solution to the grease lubricated elastohydrodynamic film thickness in an elliptical rolling contact. Proc Inst Mech Eng, Int Conf Tribol 1987;1:97–104.

[29] Hargreaves DJ, Pai R. The effect of the effective viscosity of grease on the elastohydrodynamic film thickness. Proc Aust Soc Sugar Cane Technol 2002;24:358–61.

[30] Hurley S, Cann PM. Grease composition and film thickness in rolling contacts. NLGI Spoke 1999;63(4):12–22.

[31] Kimura Y, Tama-shi N, Endo T, Dong D. EHL with grease at low speed. In: Luo J, et al. editors. Advanced Tribology, Proceedings of CIST2008 & ITS-IFToMM2008. Beijing, China, Springer; 2010. p. 15–19.

[32] Cousseau T, Björling M, Graca B, Campos A, Seabra J, Larsson R. Film thickness in a ball-on-disk contact lubricated with greases, bleed oils and base oils. Paper 3202. In: Proceedings of the 15th international conference on experimental mechanics, Porto, Portugal; 22–27 July 2012. p. 845.

[33] Jablonka K, Glovnea R, Bongaerts J. Evaluation of EHD films by electrical capacitance. J Phys D: Appl Phys 2012;45(385301):8.

[34] Jablonka K, Glovnea R, Bongaerts J, Morales-Espejel GE. Comparative measurements of EHD film thickness in ball-on-flat rig and rolling element bearing. In: Proceedings of the STLE 67th annual meeting, St. Louis, USA; 2012.

[35] Cann PM. Starvation and reflow in a grease-lubricated elastohydrodynamic contact. STLE Tribol Trans 1996;39(3):698–704.

[36] Cann PM, Spikes HA. The behaviour of polymer solutions in concentrated contacts: immobile surface layer formation. STLE Tribol Trans 1994;37(3):580–6.

[37] Smeeth M, Spikes HA, Gunsel S. Boundary film formation by viscosity index improvers. STLE Tribol Trans 1996;39(3):726–34.

[38] Kauzlarich JJ, Greenwood JA. Elastohydrodynamic lubrication with Herschel–Bulkley model greases. ASLE Trans 1972;15(4):269–77.

[39] Jonkisz W, Krzeminski-Freda H. Pressure distribution and shape of an elastohydrodynamic grease film. Wear 1979;55:81–9.

[40] Dong D, Qian X. A theory of elastohydrodynamic grease-lubricated line contact based on a refined rheological model. Tribol Int 1988;21(5):261–7.

[41] Bordenet L, Dalmaz G, Chaomleffel J-P, Vergne F. A study of grease film thickness in elastorheodynamic rolling point contacts. Lubr. Sci. 1990;2:273–84.

[42] Hamrock B, Dowson D. Isothermal elastohydrodynamic lubrication of point contacts. Part III – fully flooded results. Trans ASME, J Lubr Technol 1977;99(2):264–76.

[43] Walther C. The evaluation of viscosity data. Erdöl und Teer 1931;7:382–4.

[44] Renshaw TA. Effects of shear on lithium greases and their soap phase. Ind Eng Chem 1955;47(4):834–8.

[45] Bondi A, Caravath AM, Moore RJ. Basic factors determining the structure and rheology of lubricating greases. NLGI Spoke 1950;13(12):12–8.

[46] Bondi A, Caruso JP, Fraser HM, Smith JD, Abrams ST, Cravath AM, et al. Developments in the field of soda base greases. In: 3rd World Petroleum Congress; 1951. p. 373–395.

[47] Poon SY. Experimental study of grease in elastohydrodynamic lubrication. Trans ASME, J Lubr Technol, 94; 1972; 27–34.

[48] Cen H, Lugt PM, Morales-Espejel GE. On the film thickness of grease lubricated contacts at low speeds. Submitted to STLE Tribol Trans 2014.

[49] Dawson PH. Effect of metallic contact on the pitting of lubricated rolling surfaces. J Mech Eng Sci 1962;4(1):16–21.

[50] Lubrecht AA, Mazuyer D, Cann P. Starved elastohydrodynamic lubrication theory: application to emulsions and greases. C R Acad Sci – Ser IV, Phys Astrophys 2001;2(5):717–28.

[51] Cen H, Lugt PM, Morales-Espejel GE. Film thickness of mechanically worked lubricating grease at ultra low-speeds. STLE Tribol Trans 2014, in press.